Supplement of "Winter observations of $ClNO_2$ in northern China: Spatiotemporal variability and insights into daytime peaks"

by Men Xia et al.,

Table of Contents

Table captions

Figure captions

Section S1: technical details of N_2O_5 and $ClNO_2$ measurements

The detailed principle and description of technical aspects of the Q-CIMS, e.g., measures to minimize the inlet interference of N_2O_5 and $ClNO_2$, are available in the previous studies (Tham et al., 2016; Wang et al., 2016; Xia et al., 2020). Here we present the isotopic analysis of $ClNO_2$ signals and the normalized sensitivity of N_2O_5 and $ClNO_2$.

S1.1. Identification of $ClNO_2$ and N_2O_5

Fig. S2 shows an example of the CIMS spectrum during the daytime-$ClNO_2$ event on 28 December 2017 in Wangdu. The primary ions, I^- and $I(H_2O)^-$, were recorded at 127 atomic mass unit (a.m.u.) (Fig. S2b) and 145 a.m.u. (Fig. S2c), respectively. The analytes, $ClNO_2$ and N_2O_5, were recognized as $I^{35}ClNO_2^-$ (208 a.m.u., Fig. S2d), $I^{37}ClNO_2^-$ (210 a.m.u., Fig. S2d), and $IN_2O_5^-$ (235 a.m.u.), respectively on the Q-CIMS spectrum. Before each campaign, we calibrated the mass so that the peak of N_2O_5 and $ClNO_2$ signals points to 235.0 and 208.0. Manual scans of the mass spectrum (30~300 a.m.u.) were performed every day during the ambient sampling, in which the signals of I^-, $I(H_2O)^-$, $I^{35}ClNO_2^-$, $I^{37}ClNO_2^-$, and $IN_2O_5^-$ were recorded. The daily manual check of the peak shape and peak position ensures accurate identifications of the primary ions and analytes in this study. To further ensure the identity of $ClNO_2$, we compared the ratio of 208 a.m.u. and 210 a.m.u. signals during the ambient sampling and calibrations (Fig. S3). As for N_2O_5, field measurements with higher mass resolutions showed no interference (Breton et al., 2018), and there is no known interference of N_2O_5 reported in the literature.

S1.2. Quantification of $ClNO_2$ and N_2O_5

This section presents the sensitivity issues, detection limits, and uncertainty analysis of the Q-CIMS measurements. The detection limits of $ClNO_2$ and N_2O_5 (3σ, 5-min) are shown in Table S1. A detailed description of the uncertainty of N_2O_5 and $ClNO_2$ measurements (~19 %) is available in Xia et al. (2020). The sensitivity issues are introduced as follows.

On-site calibrations of $ClNO_2$ and N_2O_5 are referred to section 2.2 in the main text. The mixing ratios of $ClNO_2$ and N_2O_5 were calculated using the normalized sensitivity, which is essential to compensate for the potential changes in primary ions. The normalized sensitivity of $ClNO_2$ and N_2O_5 is defined as the signal ratio of 208 a.m.u. to 145 a.m.u. ($I(H_2O)^-$) and 235 a.m.u. to 145 a.m.u. in the presence of 1-pptv $ClNO_2$ or N_2O_5, respectively. For example, a normalized sensitivity of 1.3×10^{-5} Hz/Hz/pptv of N_2O_5 indicates that the sensitivity of N_2O_5 is 1.3 Hz/pptv in the presence of 10^5 Hz of $I(H_2O)^-$ signals. Results show that the normalized sensitivities of $ClNO_2$ and N_2O_5 are stable within each campaign (Fig. S5). A discrepancy of normalized sensitivities of $ClNO_2$ and N_2O_5 exists among different campaigns, owing to unknown factors, e.g., changes of instrument status after transport. We found a negative dependence of the normalized sensitivity of N_2O_5 on RH during the on-site calibrations (Fig. S4). While there is no obvious dependence of the normalized sensitivity of $ClNO_2$ on RH.

Table S1. Sensitivities and detection limits of N_2O_5 and $ClNO_2$ measurements.

Site	Wangdu	Beijing	Mt. Tai
Detection limit of N_2O_5[1]	7.3 ± 1.0	6.9 ± 1.6	6.9 ± 2.3
Detection limit of $ClNO_2$[1]	5.3 ± 1.3	3.9 ± 1.9	3.8 ± 1.9
Normalized sensitivity of N_2O_5[2]	(1.3 ± 0.2) × 10^{-5}	(2.2 ± 0.2) × 10^{-5}	(1.7 ± 0.2) × 10^{-5}
Normalized sensitivity of $ClNO_2$[2]	(9.1 ± 1.9) × 10^{-6}	(1.8 ± 0.2) × 10^{-5}	(1.4 ± 0.2) × 10^{-5}

[1]. The detection limits (unit: pptv) are derived from the standard deviations of the signals

(3σ in 5-min data) in the background testing.

[2] The unit for the normalized sensitivity is Hz/Hz/pptv.

Table S2. The measured species and instruments in the field campaigns.

Measured species	Instruments	Detection limits	Time resolution
N_2O_5, $ClNO_2$	Q-CIMS, THS	5~8 pptv	10 s
NO, NO_2	42i-TL, Thermo Scientific	0.06 ppbv	1 min
NO_y	EC9843, Ecotech	0.1 ppbv	1 min
CO	48i, Thermo Scientific	4 ppbv	1 min
SO_2	43C, Thermo Scientific	0.1 ppbv	1 min
O_3	49i, Thermo Scientific	0.5 ppbv	1 min
HONO	LOPAP-03, QUMA	5 pptv	1 min
jNO_2	Filter Radiometer, metcon	4×10^{-5} s^{-1}	10 s
$PM_{2.5}$	TEOM 1400A, Thermo Scientific	1 μg m^{-3}	1 min
VOCs	GC-MS/FID, Chromatotec Group	~10 pptv	1 h
PNSD	WPS 1000XP, MSP Corp.	1 particle cm^{-3}	1 min
NH_4^+, Cl^-, NO_3^-, SO_4^{2-}	ACSM, Aerodyne Research Inc.	0.01~0.06 μg m^{-3}	10 min
	MARGA, Metrohm AG	0.01~0.06 μg m^{-3}	1 h

Table S3. Input parameters of the box model for case studies with high concentrations of daytime $ClNO_2$.

No.	Parameter	Wangdu	Beijing	Mt. Tai
1	$PM_{2.5}$ (μg m^{-3})	162.23±90.64[1]	116.47±69.33	66.65±37.11
2	RH (%)	69.22±7.67	33.78±14.67	85.52±14.43
3	Temp (°C)	-1.95±2.77	1.43±4.17	9.88±1.53
4	NO (ppbv)	87.84±89.48	25.62±27.52	0.36±0.35
5	NO_2 (ppbv)	39.58±7.68	37.24±19.28	3.83±2.04
6	O_3 (ppbv)	3.74±2.71	12.37±10.57	59.79±8.6
7	CO (ppbv)	3156.92±1240.79	1881.1±898.67	623.8±213.84
8	SO_2 (ppbv)	11.87±3.28	6.22±2.25	2.13±1.85
9	N_2O_5 (ppbv)	0.02±0.01	0.07±0.11	0.01±0.02
10	$ClNO_2$ (ppbv)	0.33±0.28	0.16±0.17	0.26±0.21
11	HONO (ppbv)	4.13±2.41	1.02±0.46	0.13±0.09
12	jNO_2 ($\times10^{-3}$ s^{-1})	0.59±0.86	0.95±1.43	0.88±1.23
13	C2H6	16.13±8	0.96±0.42	3.93±0.45
14	C2H4	1.93±1.42	0.43±0.18	1.1±0.53
15	C3H8	6.48±2.96	6.03±0.9	1.94±0.52

16	C3H6	5.53±4.27	2.02±0.81	0.15±0.09
17	IC4H10	1.93±0.51	0.79±0.28	0.39±0.16
18	NC4H10	3.84±1.14	1.18±0.69	0.74±0.33
19	C2H2	6.04±3.53	0.38±0.36	2.1±0.32
20	TBUT2ENE	0.27±0.26	-	0.01±0.01
21	BUT1ENE	0.77±0.61	0.04±0.01	0.03±0.02
22	CBUT2ENE	0.14±0.05	0.15±0.04	0.01±0.01
23	Cyclopentane	2.67±0.7	0.02±0	0.04±0.02
24	IC5H12	0.21±0.17	-	0.35±0.18
25	NC5H12	1.53±0.51	-	0.25±0.11
26	Freon114	0.03±0	-	0.02±0
27	CH3CL	0.45±0.06	-	1.1±0.31
28	C4H6	0.27±0.23	0.04±0.01	0.02±0.01
29	CH3BR	0.01±0	-	0.06±0.06
30	Freon11	0.4±0.04	-	0.26±0.01
31	PENT1ENE	0.18±0.15	0.02±0.01	0.01±0.01
32	TPENT2ENE	0.14±0.11	-	-
33	C5H8	0.13±0.12	0.01±0	0.01±0.01
34	Freon113	0.07±0	0.07±0	0.08±0
35	CH2CL2	1.64±0.98	-	0.45±0.08
36	M2PE	0.44±0.15	-	0.06±0.03
37	M3PE	0.36±0.09	-	0.04±0.02
38	M22C4	0.05±0.01	-	-
39	M23C4	0.07±0.03	-	-
40	NC6H14	0.62±0.23	0.22±0.05	0.09±0.05
41	MACR	0.03±0.02	0.13±0	2.91±1.29
42	2,4-Dimethylpentane	-	-	-
43	CHCL3	0.66±0.21	-	0.32±0.14
44	CH3CCL3	0.01±0	-	0±0
45	Carbontetrachloride	0.15±0.01	-	0.11±0.02
46	CHEX	0.18±0.05	0.33±0.16	-
47	M3HEX	-	0.03±0.01	-
48	MTBE	0.16±0.05	-	-
49	BENZENE	4.25±2.63	1.58±0.37	0.71±0.19
50	2,2,4-Trimethylpentan	0.07±0.03	-	0.02±0.01
51	NC7H16	0.24±0.13	0.06±0.03	0.04±0.02
52	TOLUENE	3.28±1.58	0.61±0.31	0.37±0.24
53	NC8H18	0.17±0.1	0.06±0.04	0.03±0.01
54	EBENZ	0.47±0.25	0.14±0.07	0.09±0.03
55	NC9H20	0.13±0.09	0.01±0.01	0.04±0.02
56	MXYL	1.15±0.65	0.29±0.12	0.1±0.04
57	OXYL	0.41±0.28	0.11±0.06	0.05±0.02

58	STYRENE	0.39±0.31	0.03±0.01	0.01±0.01
59	IPBENZ	0.04±0.02	-	0.01±0
60	PBENZ	0.04±0.02	0.02±0.01	0.01±0.01
61	NC10H22	0.09±0.07	0.15±0.07	0.02±0.01
62	TM135B	0.06±0.04	0.02±0.01	0.01±0.01
63	TM124B	0.16±0.12	0.06±0.02	0.02±0.01
64	TM123B	-	0.1±0.03	-
65	CH4	2000.00	2000.00	2044.15±30.31
66	HCHO	3.54±1.03	3.18±0	4.93±1.53
67	CH3CHO	2.93±0.69	2.5±0	2.17±0.52
68	C2H5CHO	0.41±0.07	0.29±0	0.17±0.07
69	CH3COCH3	2.3±0.75	2.57±0	5.11±1.7
70	C3H7CHO	0.85±0.14	0.17±0	1.5±0.47
71	BENZAL	0.18±0.03	0.16±0	0.11±0.03
72	C4H9CHO	0.27±0.04	0.04±0	0.19±0.04
73	C5H11CHO	0.12±0	0.16±0	0.13±0.04

[1] 24-h average values ± standard deviations are shown here. The names of VOCs and OVOCs are presented in MCM style. The units of VOCs and OVOCs are ppbv. "-" indicates that the parameter is not constrained in the model.

Table S4. A summary of $\gamma(N_2O_5)$ derived in the selected time periods of the winter campaigns.

Start Time	End Time	$\gamma(N_2O_5)$	$\varphi(ClNO_2)$
Wangdu			
12/17/17 1:10	12/17/17 4:20	0.0150	0.037
12/24/17 23:40	12/25/17 1:30	0.0060	0.053
Beijing			
1/20/18 3:45	1/20/18 6:05	0.0075	0.630
1/25/18 23:40	1/25/18 2:20	0.0125	0.061
1/26/18 2:50	1/26/18 6:05	0.0149	0.038
Mt. Tai			
3/9/18 18:10	3/9/18 20:00	0.0525	0.797
3/24/18 19:20	3/24/18 21:00	0.0036	0.545
3/24/18 18:00	3/25/18 2:00	0.0060	0.179
3/25/18 21:00	3/26/18 2:00	0.0118	0.273

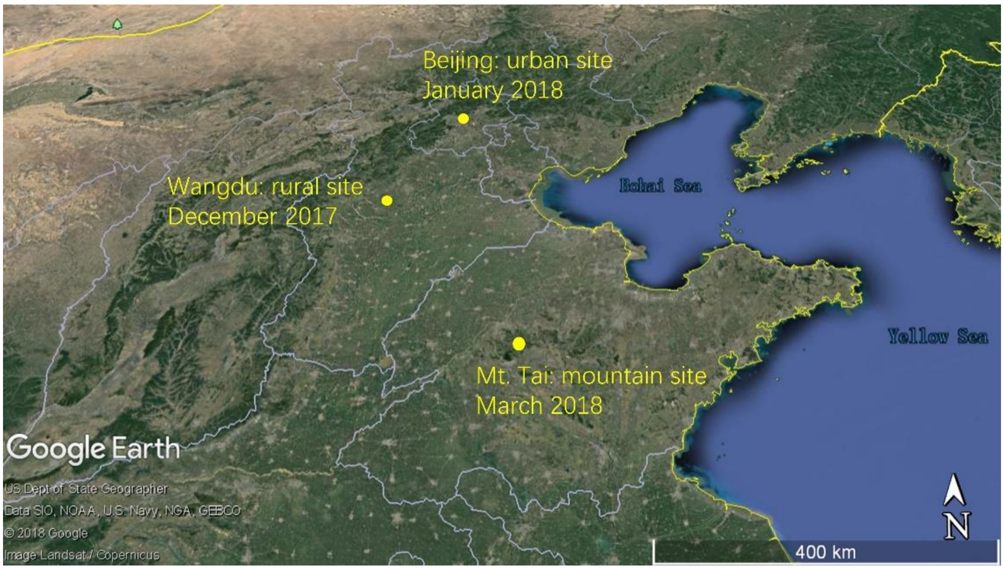

Figure S1. A map showing the three observation sites over the NCP.

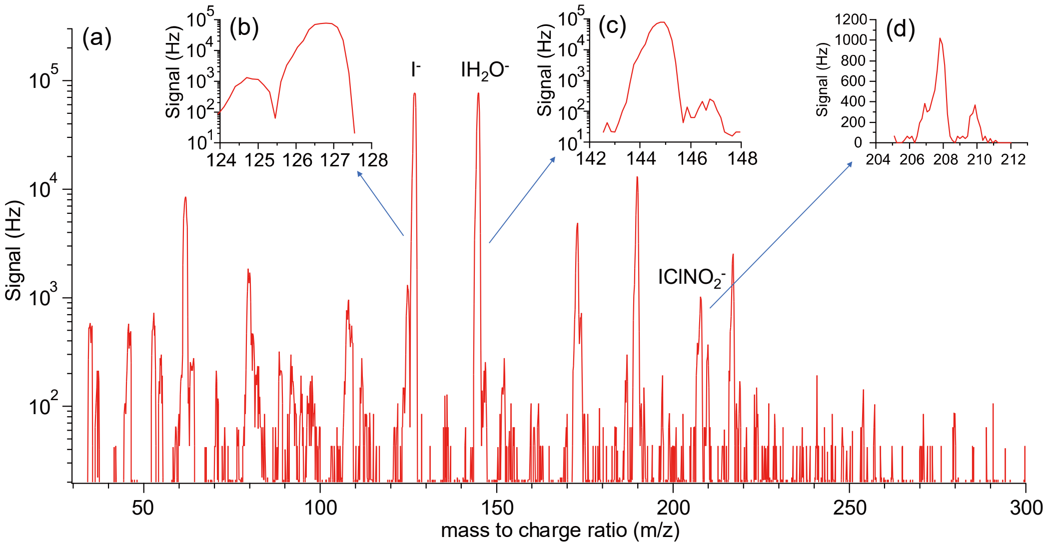

Figure S2. An example of the mass spectrum of Q-CIMS. **(a)** A full mass spectrum from 30 to 300 a.m.u. **(b)**, **(c)**, and **(d)** are expanded views of the mass spectrum for I^-, $I(H_2O)^-$, and $IClNO_2^-$, respectively.

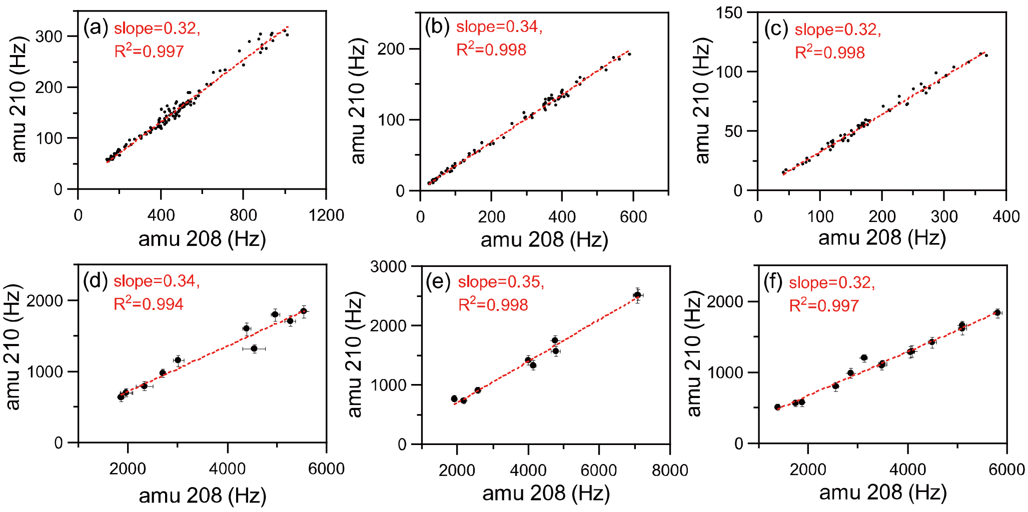

Figure S3. The signal of $I^{35}ClNO_2^-$ and $I^{37}ClNO_2^-$ during the ambient sampling and on-site calibrations. **(a)-(c)** represent the signals of 208 a.m.u. and 210 a.m.u. during the ambient observations on the daytime of 28 Dec 2017 in Wangdu, 14 January 2018 in Beijing, and 29 March 2018 in Mt. Tai, respectively. **(d)-(f)** show the respective signals of 208 a.m.u. and 210 a.m.u. during the on-site calibrations in Wangdu, Beijing, and Mt. Tai, respectively.

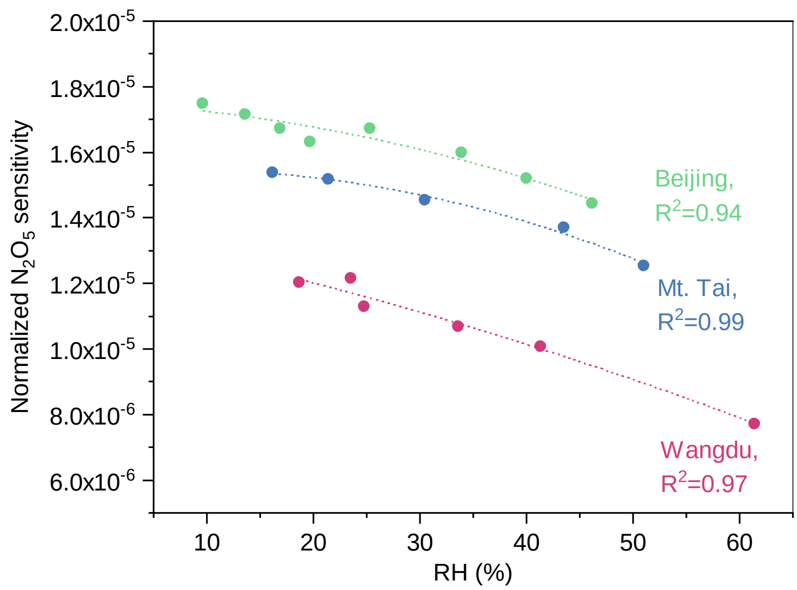

Figure S4. The dependence of normalized N_2O_5 sensitivities on RH. The dots with different colors were experiment data in Wangdu, Beijing, and Mt. Tai, respectively, which was fitted by a quadratic function in the form of $y=ax^2+bx+c$.

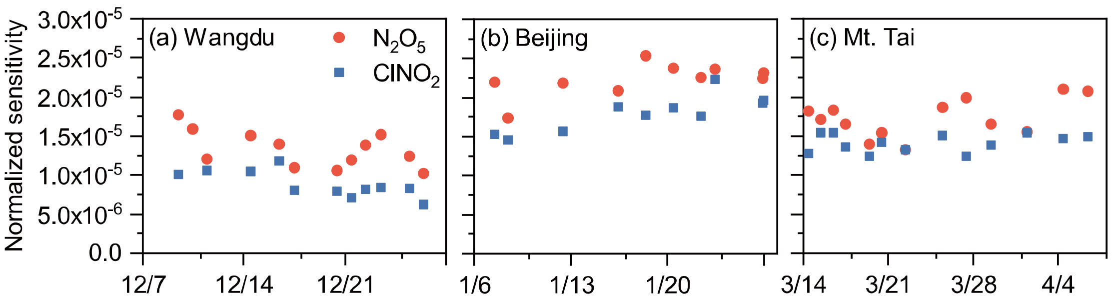

Figure S5. Summary of on-site calibrations of N_2O_5 and $ClNO_2$. The unit of the normalized sensitivity of N_2O_5 and $ClNO_2$ is Hz/Hz/pptv.

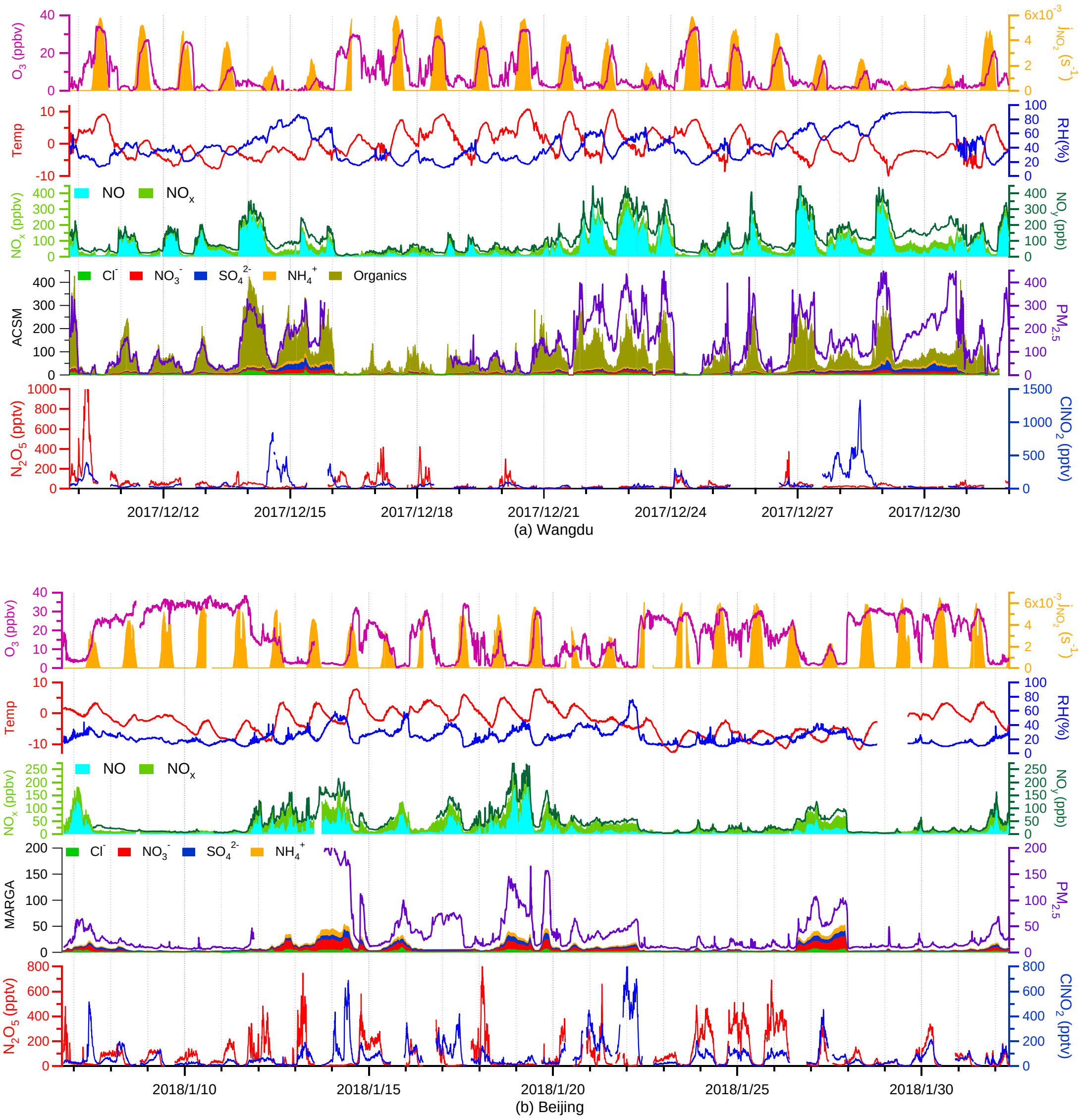

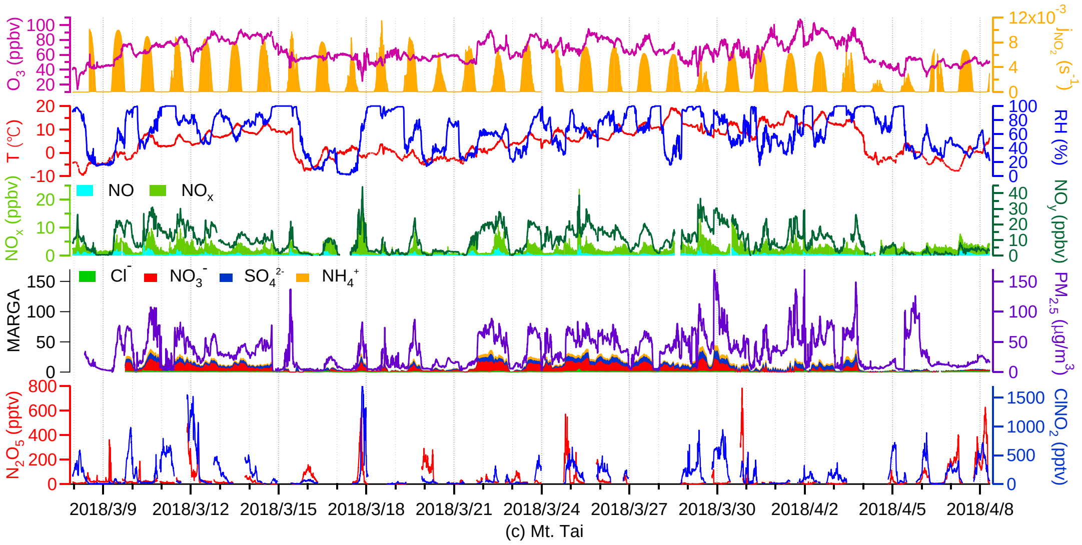

Figure S6. Time series of some observed species of **(a)** the Wangdu campaign in December 2017, **(b)** the Beijing campaign in January 2018, and **(c)** the Mt. Tai campaign in March 2018.

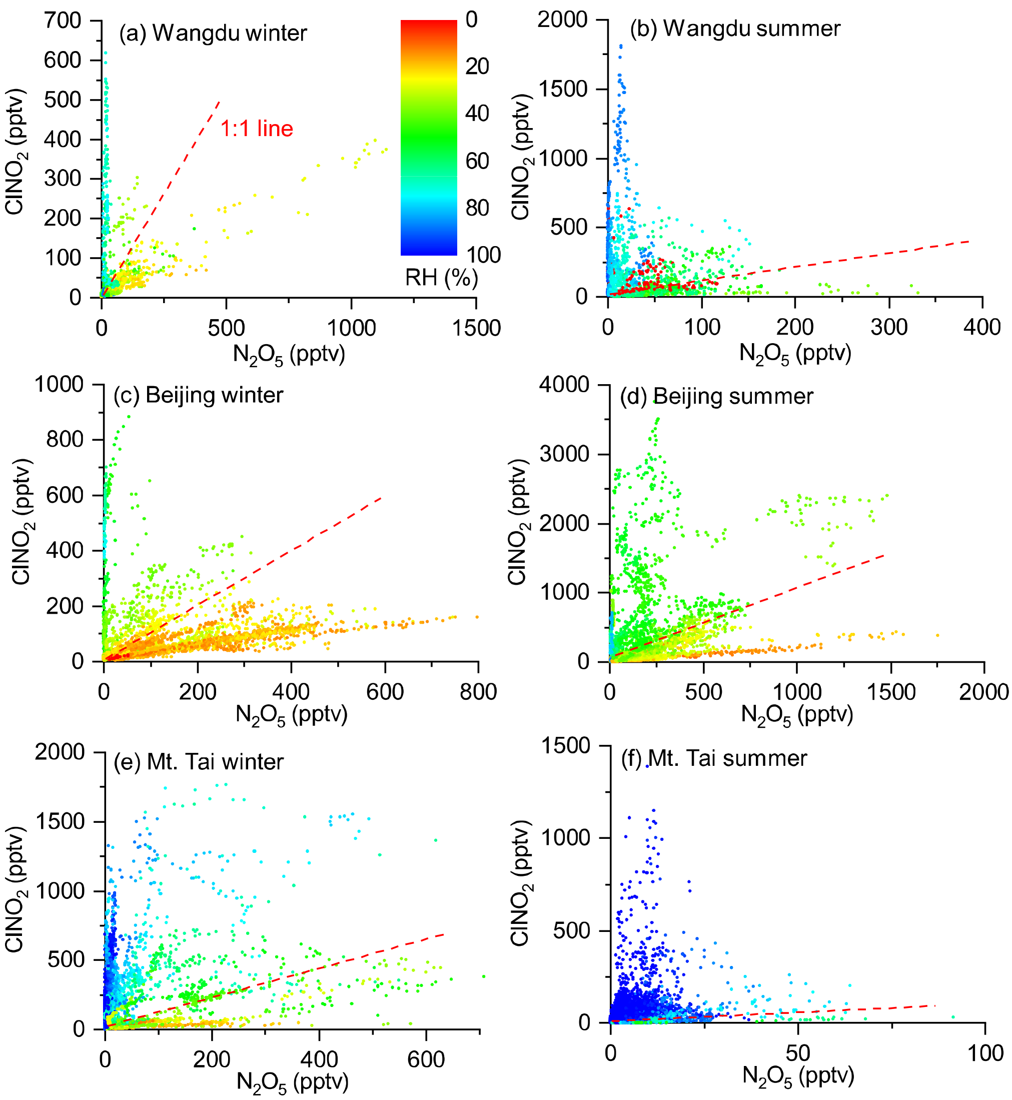

Figure S7. Nocturnal relationship of the concentrations of N_2O_5 and $ClNO_2$ in the winter and summer campaigns in Wangdu, Beijing, and Mt. Tai. The dashed line in red shows a 1:1 ratio of the concentrations of N_2O_5 and $ClNO_2$.

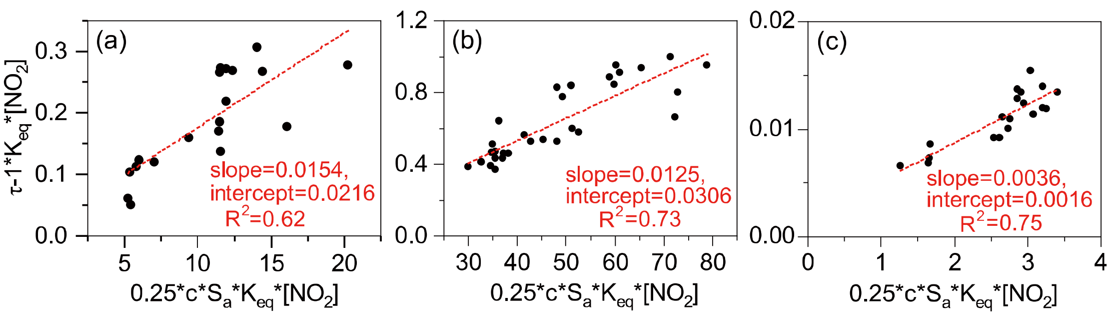

Figure S8. Examples of γ(N_2O_5) derived using the steady-state method. **(a)** 16 December 2017 in Wangdu, **(b)** 25 January in Beijing, and **(c)** 24 March in Mt. Tai.

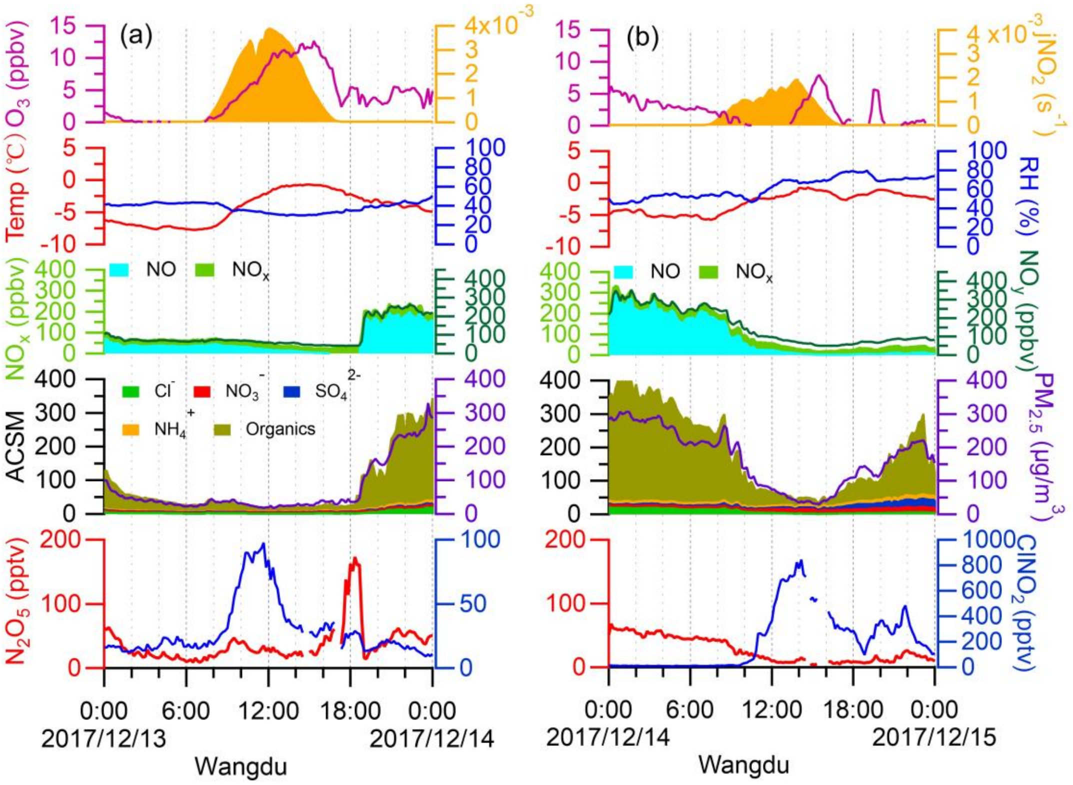

Figure S9. Examples of other daytime-$ClNO_2$ cases observed during the winter Wangdu campaign.

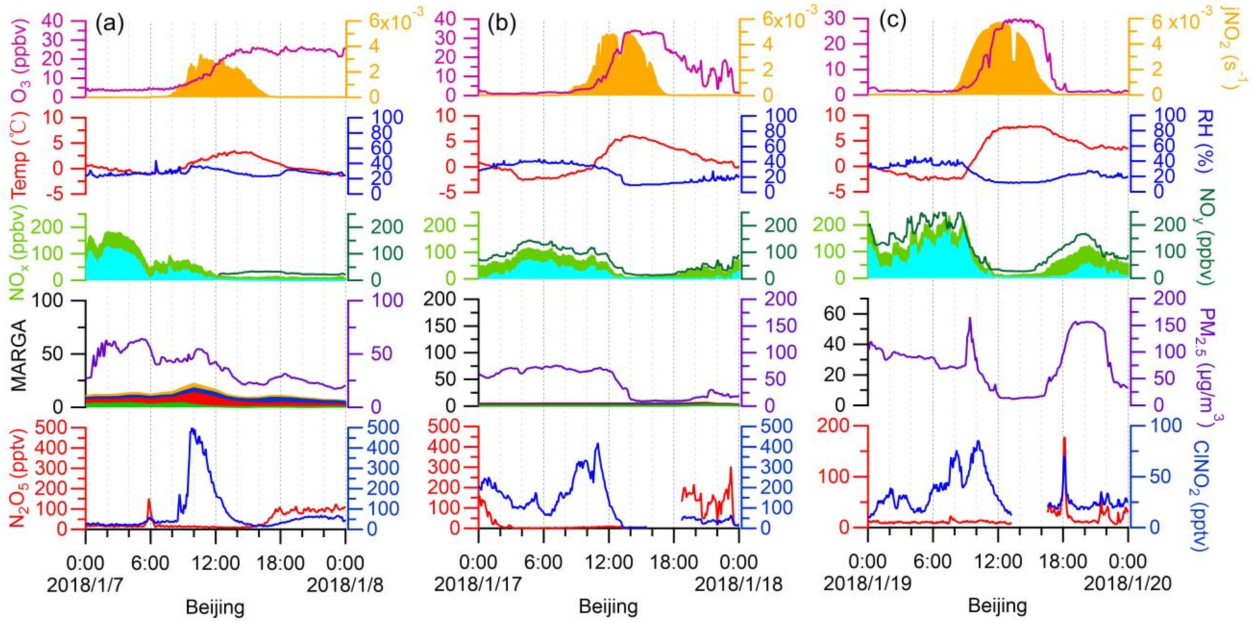

Figure S10. The same to Fig. S9 but for the winter Beijing campaign.

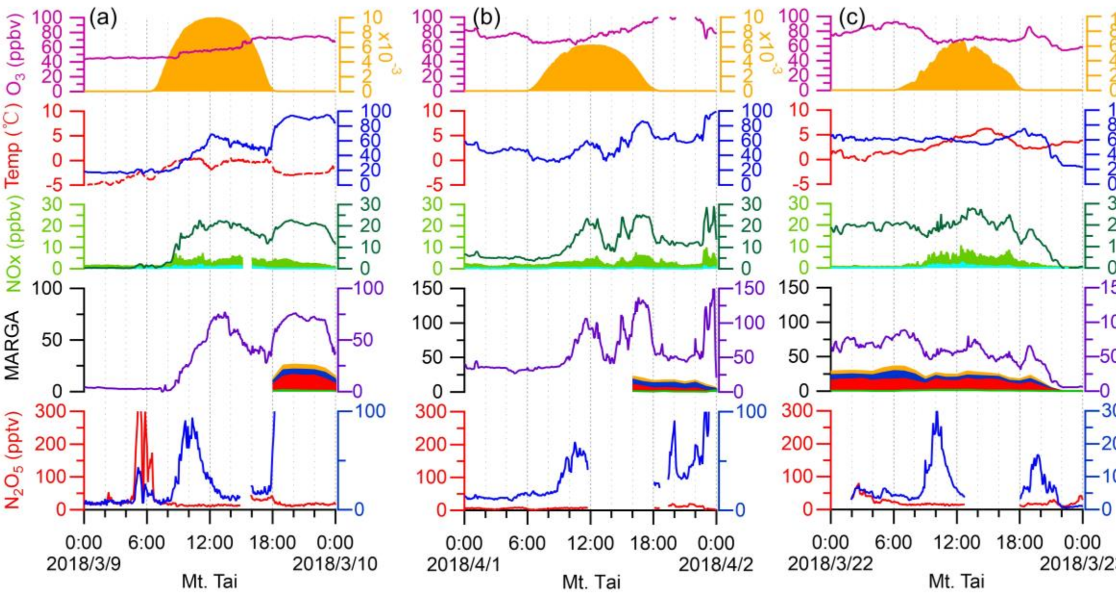

Figure S11. The same to Fig. S9 and Fig. S10 but for the winter Mt. Tai campaign.